Mass Transfer Between Immiscible Liquid Metals

ALAN D. PASTERNAK and DONALD R. OLANDER

Lawrence Radiation Laboratory, University of California, Berkeley, California

The extraction of lanthanum and barium from single falling drops of the uranium-chromium eutectic into magnesium was studied at 1,000°C. Because of the short contact times involved, the data best fit the stagnant diffusion model for lanthanum. For barium, the fraction extracted was governed by external resistance of the magnesium phase. Drop velocities were adequately represented by the Hu-Kintner correlation.

Reprocessing of spent reactor fuel is conventionally accomplished by aqueous chemical methods involving dissolution, extraction, and calcination of the fuel material. During the past fifteen years, a number of laboratories have investigated reprocessing techniques in which the fuel is treated as a liquid metal rather than in aqueous solution. These processes utilize the chemical and physical properties of fuel at elevated temperatures to achieve decontamination from fission products. Among these pyrochemical processes is liquid metal extraction.

The object of the present work was to investigate extraction kinetics in a typical uranium bearing liquid metal–immiscible solvent metal system in order to determine whether the sizable background on extraction in low temperature, aqueous-organic systems could be applied to liquids with markedly different characteristics. Properties such as density differences and interfacial tensions are orders of magnitude greater in liquid metal systems than in any combination of aqueous-organic solvents.

THE IMMISCIBLE SOLVENT PHASES: URANIUM-CHROMIUM EUTECTIC AND MAGNESIUM

Most pyrochemical processes applied to nuclear fuels involve treating uranium either as a pure liquid or as a solute in other liquid metals. Pure uranium, however, melts at 1,132°C., and operation at these elevated temperatures is difficult because of the attack of most container materials by the liquid metals. In order to retain the features characteristic of a uranium rich liquid yet reduce the experimental temperature, the eutectic alloy of uranium and chromium was employed. This binary contains 95 wt.% uranium (80 at.%), yet melts at 860°C.

Magnesium and silver are two solvents immiscible with uranium. However, silver was not used because of the rather large amounts required for extraction kinetic studies. Magnesium is a satisfactory solvent except for its high vapor pressure. At the experimental temperature of 1,000°C., the vapor pressure is 300 mm. Hg, and a means of refluxing vaporized magnesium to the extraction column had to be devised.

Because of the corrosive nature of the molten metals at 1,000°C., only the simplest equipment, with no moving parts such as valves, could be employed. The least complex contacting method which still provided some semitheoretical foundation for data interpretation was extraction from single falling drops. This technique has been employed in liquid metal-fused salt investigations at 500°C. (*10, 13*), but at 1,000°C. even the modest refinements in drop entry and recovery methods used in these studies were not feasible.

Consequently, the system consisted of a column of molten magnesium into which a small pellet of solid irradiated uranium-chromium eutectic was lowered by means of a tungsten wire. The pellet melted off the wire and fell to the bottom of the column. The fall velocity of the drops was measured. The amount of lanthanum-140 extracted was determined from the activity of the recovered magnesium ingot, and the amount of barium extracted was determined by following the decay of lanthanum-140 in the ingot.

Alan D. Pasternak is with the Lawrence Radiation Laboratory, Livermore, California.

THE TRANSFERRING SOLUTES: LANTHANUM-140 AND BARIUM-140

The solute directly measured in the experiments was the rare earth, lanthanum-140. This nuclide is not produced directly by uranium fission but is the daughter of barium-140 which is produced with a direct fission yield of 6.4%. The decay scheme is

$$Ba^{140} \xrightarrow[12.8\ d]{\beta^-} La^{140} \xrightarrow[40.2\ hr.]{\beta^-} Ce^{140} \qquad (1)$$

The fission of uranium produces a wide range of radioactive fission products. Those nuclides which emit high energy gamma rays tend to have short half lives. Because of the long half life of its parent, however, the 1.6 megavolt photon from lanthanum-140 decay dominates the gamma-ray spectrum of uranium which has been cooled for several days. The intensity of this photopeak served as a measure of the lanthanum-140 concentration in the solvent metals.

Since the lanthanum activity depends upon the 12.8 day half life of its precursor barium-140, the amount of barium extracted can be determined by following the decay of the lanthanum after an experiment. This can be qualitatively illustrated by considering the two extreme cases. If only lanthanum were extracted, its activity would decay with a half life of 40.2 hr. However, if only barium were extracted, the lanthanum activity would initially increase from zero to some maximum and then decrease, asymptotically approaching the 12.8 day half life of the barium precursor. The decay of the lanthanum is governed by the well-known relation for batch decay of a two member chain:

$$\frac{a_{La}}{a^o_{La}} = \frac{e^{-\lambda_{Ba}t}}{F} + \left(1 - \frac{1}{F}\right) e^{-\lambda_{La}t} \qquad (2)$$

where the parameter F depends upon the initial ratio of the two nuclides:

$$F = \left(\frac{N^0_{La}}{N^0_{Ba}}\right)_{Mg} \frac{\lambda_{La} - \lambda_{Ba}}{\lambda_{Ba}} \qquad (3)$$

If the initial ratio is such that F is unity, the lanthanum activity decays with the half life of the barium precursor. This situation is known as secular equilibrium and for the chain of Equation (1) is attained after about twelve days in uranium irradiated for two days.

The initial lanthanum to barium atom ratio in the magnesium after extraction is related to the same ratio in the uranium-chromium pellet before extraction and the fractions extracted of each of the species by

$$\left(\frac{N^0_{La}}{N^0_{Ba}}\right)_{Mg} = \left(\frac{N_{La}}{N_{Ba}}\right)_{\substack{U\text{-}Cr \\ initial}} \frac{f_{La}}{f_{Ba}} \qquad (4)$$

The atom ratio in the pellet before extraction corresponds to secular equilibrium:

$$\left(\frac{N_{La}}{N_{Ba}}\right)_{\substack{U\text{-}Cr \\ initial}} = \frac{\lambda_{Ba}}{\lambda_{La} - \lambda_{Ba}} \qquad (5)$$

When one substitutes Equation (5) into Equation (4) and compares the result to Equation (3), the measured value of F is seen to equal the ratio of the fractions extracted:

$$F = \frac{f_{La}}{f_{Ba}} \qquad (6)$$

In accordance with Equation (2), a plot of (a_{La}/a^o_{La}) exp $(\lambda_{Ba}t)$ vs. exp $[-(\lambda_{La} - \lambda_{Ba})t]$ for the magnesium ingot after extraction should yield a straight line with an intercept of $1/F$. A typical plot of this type is shown on Figure 1. In this experiment, the fraction of barium extracted was one quarter of the fraction of lanthanum removed from the pellet. The latter is obtained from the ratio of the lanthanum-140 activity in the magnesium ingot immediately after extraction to that in the pellet before the experiment.

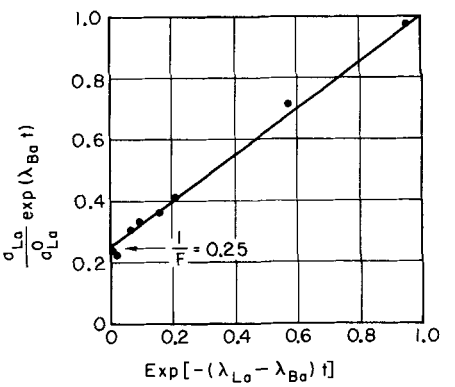

Fig. 1. F plot for the magnesium ingot after extraction for run No. 10.

EXPERIMENTAL PROCEDURE

The experiments were performed in the apparatus shown in Figure 2. The extraction column was a graphite crucible with a 31 in. overall length, 1¼ in. O.D., and 9/16 in. I. D. The crucible was closed at the bottom by a machined graphite screw plug, which held magnesium without any leakage. A 23 in. long reflux column, also of graphite, was placed directly above the extraction column. The reflux column condensed magnesium vapor and returned it to the extraction column,

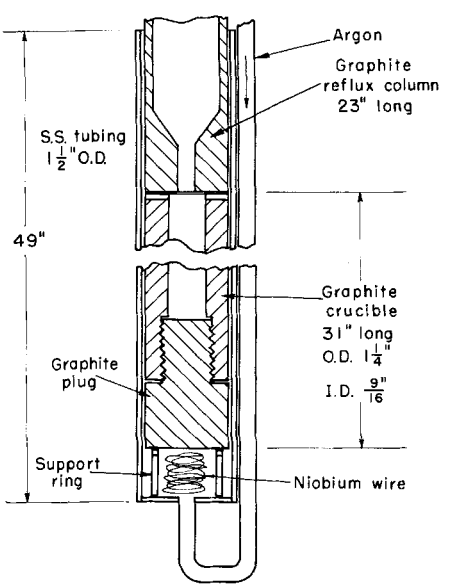

Fig. 2. Extraction column, reflux column, and sheath.

thus minimizing magnesium losses. Both extraction and reflux columns were placed in a stainless steel sheath which was flushed with an inert gas during the experiments. The sheath containing the extraction column was supported in a hinged vertical tube resistance furnace by means of a flange. The velocity of the uranium-chromium drop as it fell through the magnesium column was measured by three collimated scintillation detectors. Figure 3 shows the graphite crucible, reflux column, magnesium charge, and dropping stick against a schematic design of the furnace, gamma-ray scintillation detectors, and high-speed recorder. Figure 4 shows a typical trace from the high-speed recorder. Drop velocities were calculated between the top and middle and the middle and bottom detectors. Velocities in the second interval were about 15% higher than those measured in the top of the column. The former were taken as the terminal velocities.

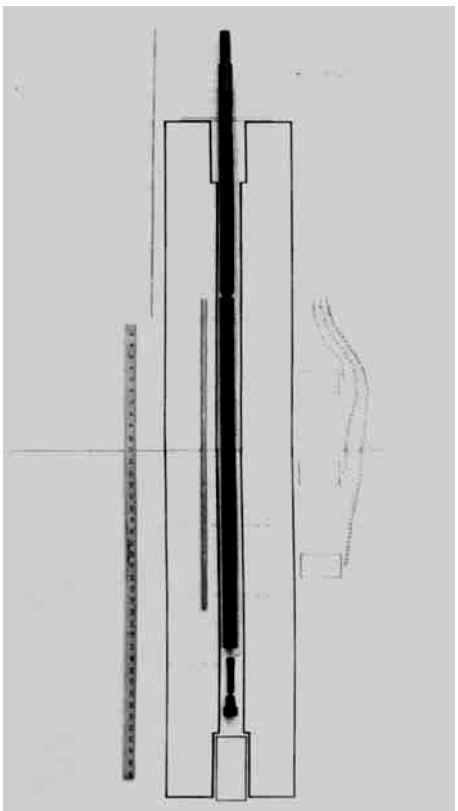

Fig. 3. Schematic of experimental arrangement.

A positive temperature gradient was maintained in the column in order to minimize natural convection currents in the magnesium. The molten magnesium temperature ranged from 980°C. at the bottom of the column to 1,020°C. at the top.

Magnesium was obtained from the United Mineral and Chemical Corporation in the form of ½-in. diam. sticks. Before a stick was placed in the crucible, it was cut to a length of 27½ in., and the surfaces were carefully scraped or machined to remove the oxide coat. The length of the molten magnesium column was about 60 cm.

The uranium-chromium eutectic alloy was obtained from the National Lead Company in the form of right circular cylinders ¼ in. in diameter and about ⅜ in. high. The alloy was made of depleted uranium containing about 0.2 wt.% U^{235} (natural uranium contains 0.7 wt.% U^{235}). The supplier reported the melting point as 860°C. Analysis of alloy samples showed the chromium content to be 4.28 wt.% (the eutectic alloy contains 5 wt.% chromium). Spectrographic analysis showed no constituents other than chromium and uranium. Pellets weighing from 0.1 to 0.6 g. were cut from the larger pieces with a hacksaw. A small hole was drilled through the

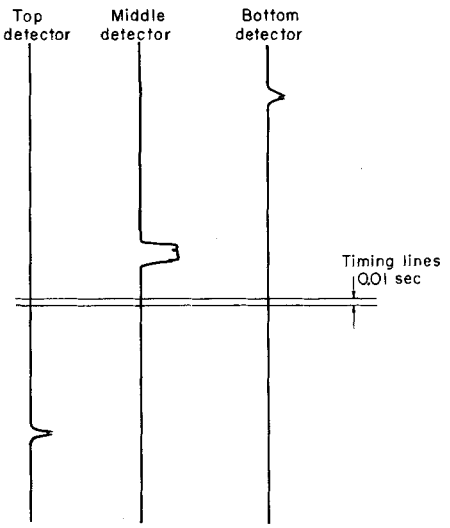

Fig. 4. Typical output of oscillograph for measurement of fall velocity.

center of each pellet. After the pellets were weighed, they were individually sealed in argon filled quartz capsules and irradiated for 48 hr. at thermal neutron fluxes of 10^{12} to 10^{13} neutrons/sq. cm./sec. The lanthanum-140 activity of the pellet before the experiment was measured on a multichannel analyzer.

In several runs, special precautions were taken to eliminate any possible oxide film on the uranium-chromium surface which would block mass transfer at the eutectic-magnesium interface. Uranium is extremely reactive, but so is magnesium. Magnesium oxide is thermodynamically more stable than uranium dioxide, and it might be expected that any uranium dioxide present on the pellet surface would be reduced as the pellet fell through the column. It is not certain, however, that this reaction could completely clean the uranium-chromium in the approximatey 1 sec. of contact time. To minimize the possibility of uranium dioxide formation on the pellet surface, four of the uranium-chromium pellets were given a protective magnesium coating prior to irradiation. The pellet was allowed to soak in molten magnesium at 750°C. for about 15 min. After cooling, the hole later used for introducing the pellet in the extraction column was then drilled through the outer magnesium layer and the pellet. The coated pellets were then sealed in argon filled quartz capsules and irradiated as before.

The pellet was prepared for introduction into the extraction column by suspending it from a tungsten wire loop at the end of a long stainless steel rod. The rod was lowered through the reflux column, through a constriction at the bottom of the reflux column (see Figure 2), and into the extraction column. The rod was lowered until the pellet was just below the molten magnesium surface. Within a few seconds, the pellet melted off the tungsten loop and fell through the column, its passage being detected by the three collimated scintillation counters placed along the column. In this way, it was certain that the pellet entered the column as a liquid drop.

The pellet fell through the molten magnesium and into a puddle of molten barium chloride about 1 in. deep contained in a graphite inner liner at the bottom of the column just above the screw plug. The inner liner is shown just above the screw plug in Figure 3. As soon as the scintillation detectors recorded the fall of the uranium-chromium drop, the furnace was immediately turned off in order to freeze the barium chloride, whose melting point (960°C.) is only 20°C. below the temperature of the bottom of the column. (Molten barium chloride is twice as dense as magnesium at 1,000°C. It is chemically stable with respect to uranium, magnesium, and lanthanum.) Thus the uranium-chromium pellet at the bottom of the crucible was separated physically from the molten

magnesium which takes longer to freeze (MP 650°C.). In this way, continued extraction after the pellet has reached the bottom of the column was prevented. In several early experiments, no puddle of barium chloride salt was used at the bottom of the column. Counting collimated 2-in. lengths of the frozen magnesium ingot after extraction showed large end effects when the pellet remained in contact with molten magnesium during the cooling period. The presence of the salt-magnesium interface prevented these large end effects.

As soon as the oscillograph recorded the passage of uranium-chromium drop, the furnace was turned off. After cooling and disassembly, the recovered magnesium ingot was placed in an argon filled dry box, and the inner liner containing the uranium-chromium pellet buried in frozen barium chloride was sawed off. The magnesium ingot, inner liner, and crucible were then examined with the multichannel analyzer for lanthanum-140.

The properties of the magnesium uranium-chromium system at 1,000°C. are shown in Table 1. A complete discussion of the sources of these data and the estimation of unknown properties are given in reference *17*. Very recently, the viscosity of uranium has been measured (*12*). The viscosity of the eutectic has been assumed to be equal to that of supercooled uranium. Diffusion coefficients were estimated by the methods of reference *16*.

TABLE 1. PROPERTIES OF THE MAGNESIUM—URANIUM-CHROMIUM EUTECTIC SYSTEM AT 1,000°C.

Property	Mg	U-Cr
Density, g/cc.	1.5	16.6
Viscosity, centipoise	0.55	8.7
Surface tension, dynes/cm.	440	1,610
Interfacial tension, dynes/cm.	1,170 (Antonov's rule) 370 (method of reference 4)	
Lanthanum distribution coefficient*	0.16	
Barium distribution coefficient*	0.0035	
Lanthanum diffusivity, sq. cm./sec. × 10^5	14.5	1.8
Barium diffusivity, sq. cm./sec. × 10^5	14.9	1.8

* Distribution coefficients on a concentration basis, magnesium to uranium-chromium.

TABLE 2. SUMMARY OF DROP VELOCITY DATA

Run No.	Drop diameter, cm.	Terminal velocity, cm./sec.	Reynolds number N_{Re}
6	0.21	46	2,660
14	0.22	68	4,010
7	0.29	77	5,960
15	0.30	73	5,900
1	0.31	71	5,970
2	0.34	65	5,890
4	0.35	63	5,980
9	0.35	68	6,520
10	0.37	73	7,300
17	0.41	73	8,100
11	0.41	68	7,590

RESULTS

Drop Velocities

A total of thirteen kinetic experiments were conducted. The measured terminal velocities for the eleven satisfactory attempts are tabulated in Table 2. The trace for run No. 12 showed a double blip at the bottom detector, and it was assumed that this drop split up. The pellets used in runs 12 and 13 (the two largest) evidently broke during the melting process, since in each case a large fragment of the drop was later found near the top of the column against the crucible wall. The drop velocities recorded in Table 2 are independent of pellet size with the exception of run No. 6 which showed a lower velocity than the others. This pellet, the smallest used, may have hit the column wall while falling.

Figure 5 compares the data with the generalized Hu and Kintner correlation (*8*). The data have been treated with the two values of interfacial tension given in Table 1. The larger value for interfacial tension gives a better fit to the generalized curve. The average of the observed terminal velocities is about 13% higher than that predicted by the correlation for the larger interfacial tension and 30% higher for the lower interfacial tension. The system studied here extends the correlation to values of the physical properties which far exceed those studied by Hu and Kintner. For the uranium-chromium-magnesium system the density difference is 15.1 g./cc. The largest density difference used in the Hu-Kintner correlation was ~ 1.95 g./cc. Interfacial tension in the uranium-chromium-magnesium system far exceeds values typical of immiscible aqueous-organic systems. The largest interfacial tension in the original correlation is 44 dynes/cm. Owing primarily to the large density difference, the terminal velocities observed in the present system (~ 65 to 75 cm./sec.) are greater than the largest observed by Hu and Kintner (~ 26 cm./sec.).

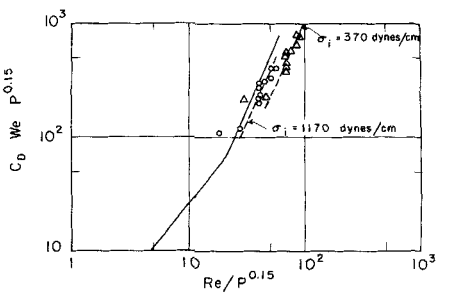

Fig. 5. Comparison of drop velocity measurements with Hu-Kintner correlation (notation that of reference *8*).

All of the velocity data are beyond the break in the Hu-Kintner correlation, which usually implies oscillation of the drops during fall. However, these authors noted that both high interfacial tension and high drop viscosity (both of which occur in the magnesium-uranium-chromium system) tend to exert a damping effect on oscillation. In particular, the extremely large interfacial tension would act to maintain a spherical drop shape. From the recent work of Wellek et al. (*20*), eccentricities of the falling drops are estimated to be ~ 1.2.

Although it cannot be determined whether the data of Table 2 represent oscillating drops, the breakup of the two largest drops indicated a critical diameter of ~ 0.5 cm. In accordance with the correlation of this parameter by Hu and Kintner, critical diameters of 1.1 cm. (for an interfacial tension of 1,170 dynes/cm.) or 0.6 cm. (for an interfacial tension of 370 dynes/cm.) are expected. If drops of diameters less than 0.4 cm. were not oscillating, the entire regime from incipient oscillation to complete disintegration must have occurred in the diameter range from 0.4 to 0.5 cm.

Solute Extraction

Table 3 lists the results of the ten experiments performed. For each solute, the fraction extracted is related to the overall mass transfer coefficient by

$$f = 1 - \exp\left(-\frac{6}{d}Kt\right) \approx \frac{6}{d}Kt \qquad (7)$$

When one assumes that the resistances in each phase are additive, then

$$\frac{1}{K} = \frac{1}{k_i} + \frac{1}{mk_e} \qquad (8)$$

The experimental external coefficients show more scatter than the internal coefficients because the former are more sensitive to the barium fraction extracted, which is not as precisely measured as that for lanthanum.

The low values of the internal coefficients suggest the existence of an interfacial resistance, which would most probably result from oxide contamination. However, the data of Table 3 show no significant difference between experiments with pellets coated or uncoated with magnesium prior to irradiation. This suggests that the mass transfer coefficients are representative of true phase resistances, although the possibility that the procedure of soaking the uranium-chromium pellets in liquid magnesium did not succeed in removing oxide at the interface cannot be discarded.

TABLE 3. EXTRACTION RESULTS

Run	d, cm.	f_{La}	F	$f_{Ba} \times 10^3$	$k_i \times 10^3$, cm./sec.			k_e, cm./sec.	
					Exp	H-B†	Stag†	Exp	Higbie
6	0.21	0.145	6.7	21.8	4.7	20	4.4	0.18	0.19
14*	0.22	0.148	14.3	10.4	8.6	29	5.0	0.11	0.23
7	0.29	0.104	7.2	14.5	7.0	37	5.3	0.26	0.21
15*	0.30	0.039	9.1	4.2	2.7	38	5.2	0.08	0.21
8	0.32	0.049	5.3	9.2	3.0	34	4.9	0.17	0.18
9	0.35	0.011	7.2	1.6	0.7	38	5.0	0.03	0.18
16*	0.37	0.049	14.3	3.5	4.9	40	5.2	0.07	0.18
10	0.37	0.061	4.0	15.3	4.6	41	5.1	0.38	0.18
17*	0.41	0.076	6.0	12.7	6.7	43	5.2	0.32	0.17
11	0.41	0.043	11.1	3.9	4.0	41	4.8	0.08	0.17

* Pellets coated with magnesim prior to irradiation.
† Based upon solutions for zero external resistance. The Handlos and Baron results were obtained from the numerical computation of reference *14*.

Since the diffusion coefficients of the two solutes are very nearly the same in each solvent (Table 1), the individual coefficients should be the same for barium and lanthanum. The overall coefficients differ only because of the fortyfold difference in the distribution coefficients. The equation which results from combining Equations (7) and (8) can be applied to the extraction data for both barium and lanthanum. From the fractions of the two solutes extracted in each experiment, external and internal coefficients have been calculated and listed in Table 3 under the heading experimental. Use of these values in Equation (8) shows that lanthanum extraction is 85% controlled by internal transfer, and barium extraction is 89% controlled by the external resistance.

Models of internal transfer which have been employed in drop extraction studies are based on stagnant diffusion, internal circulation (*11*), a type of eddy diffusion (*6*), and most recently, an explicit recognition of oscillation (*1*, *19*). External resistance has been treated primarily by the penetration model of Higbie (*7*), although the correlations of Garner et al. (*3*) and Griffith (*5*) have also been used. The experimental internal coefficients are compared with those predicted by the Handlos and Baron model in Table 3. The experimental results are low by factors of 3 to 10. The internal coefficients are in fair agreement with the predictions of the stagnant drop model. In both of these models, the external coefficients agree fairly well with the predictions of the Higbie theory:

$$k_e = 2\left(\frac{D_e u}{\pi d}\right)^{1/2} \qquad (9)$$

Since the stagnant drop calculation appears promising for this system, it is of interest to investigate the assumption of additivity of resistances, upon which the results of Table 3 are based. The additivity assumption involved in the comparison of the experimental and theoretical results in Table 3 enters in the following manner. It has been assumed that the fraction extracted can be calculated from individual coefficients by Equations (7) and (8). The internal coefficient in Equation (8), however, is computed for the case of no external resistance. The effect of external resistance on the extraction is approximated by the second term on the right of Equation (8). For drop extraction systems in general, and at short contact times in particular, the internal coefficient is both time dependent and a function of the external resistance. These characteristics render the concept of an internal mass transfer coefficient more of a complication than an aid in data interpretation.

A more direct approach to the analysis of the experimental data is to assume a model for internal transfer in the form of a conservation principle and to solve the resulting partial differential equation for the fraction extracted as a function of contact time and the external resistance parameter The latter is obtained from independent theoretical considerations and enters as a boundary condition on the conservation equation for the interior of the drop. Incorporation of the external resistance boundary condition into the three models of internal transfer mentioned previously has been accomplished by the eigenvalue expansion technique (*2*, *15*, *18*).

Because of the reasonable agreement between the experimental results of Table 3 and the stagnant diffusion

prediction, only this mode of internal transfer will be considered. The solution to the problem of diffusion in a sphere with the appropriate boundary conditions reflecting the finite external resistance has been obtained by Newman (*15*) in terms of an eigenvalue expansion. This solution is very inconvenient for the present study because the short contact times require a large number of terms of the series to be retained. In addition, only a limited number of the constants have been evaluated. A short-time approximation to the same problem, obtained by the Laplace transform method, is derived in reference *17*. The result is

$$f = \frac{6}{\sqrt{\pi}}\left(\frac{b}{b-1}\right)^2 \sqrt{\tau} - 3\left(\frac{b}{b-1}\right)\tau - 3\left(\frac{b}{b-1}\right)^2 \left(\frac{1-g}{b-1}\right) \quad (10)$$

where

$$g = e^{(b-1)^2\tau}\,\mathrm{erfc}\,[(b-1)\sqrt{\tau}] \quad (11)$$

$$b = \frac{amk_e}{D_i} \quad (12)$$

and τ is the dimensionless time

$$\tau = \frac{D_i t}{a^2} \quad (13)$$

as $(b-1)\sqrt{\tau} \to \infty$, $g \to 0$, and Equation (10) reduces to

$$f = \frac{6}{\sqrt{\pi}}\sqrt{\tau} - 3\left(\tau + \frac{1}{b}\right) \quad (14)$$

Although Equations (10) and (14) are in principle short-time approximations, they are valid over a very large range At a value of τ required for 90% extraction, for example, the fraction extracted from Equation (14) is within 0.2% of the value given by the exponential expansion. There is certainly no restriction on the use of Equations (10) or (14) for the results obtained in this study and, in fact, for stagnant diffusion analyses of nearly all of the drop extraction data is the literature. The theoretical internal coefficients for stagnant diffusion in Table 3 were computed from Equation (14) with $b = \infty$, and Equation (7), in which K was replaced by k_i.

Limiting cases of Equation (10) can be obtained for large or small values of the parameter $(b-1)\sqrt{\tau}$. For solute barium, the parameter b can be calculated from the distribution coefficient and diffusivity in uranium-chromium from Table 1 as

$$b_{Ba} = 96dk_e \quad (15)$$

The external coefficients were calculated from Equation (9) and are listed in the last column of Table 3. The values of $(b_{Ba}-1)\sqrt{\tau}$ are less than 0.15 for all experiments, and a three-term Taylor series expansion of Equation (11) is adequate. When inserted into Equation (10) there results

$$f_{Ba} = 3b_{Ba}\tau \quad (16)$$

This is just the expression for the fraction extracted under conditions of complete external control when the contact time is short. It does not depend upon the model chosen for internal mass transfer.

For lanthanum, values of the parameter b are given by

$$b_{La} = 4{,}400dk_e \quad (17)$$

The parameter $(b_{Le}-1)\sqrt{\tau}$ is no smaller than 6, which permits the function g to be replaced by 0. In addition, the minimum value of b_{La} is 180, and $b_{La}/(b_{La}-1)$ can be replaced by unity. In this case, Equation (10) reduces to Equation (14), which can be rewritten as

$$f_{La} = \left[\frac{6}{\sqrt{\pi}} - 3\left(\frac{1+b_{La}\tau}{b_{La}\sqrt{\tau}}\right)\right]\sqrt{\tau} \quad (18)$$

In the experiments conducted here, the values of b_{La} and τ were such that the second term in the brackets of Equation (18) was always less than 15% of the first term and, in addition, was constant to within 4%. Thus it has been replaced by its average value for the ten experiments on Table 3, and Equation (18) is written as

$$f_{La} = 2.9\sqrt{\tau} \quad (19)$$

Equations (16) and (19) represent theoretical predictions of the fraction of each solute extracted, based upon molecular diffusion within the drop coupled with an external resistance given by Higbie's model. The predictions depend upon the measured distribution coefficients of the two solutes, the measured velocities, and the estimated diffusion coefficients in the two solvent phases.

The experimental lanthanum data are compared with the predictions of Equation (19) on Figure 6. The scatter

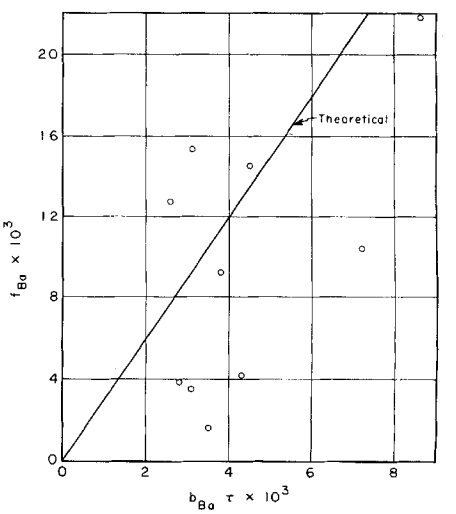

Fig. 6. Comparison of lanthanum extraction with molecular diffusion model with external resistance.

of the experimental points is due in part to the use of the single drop technique, which is not subject to the smoothing tendency of extraction measured after the passage of many drops through the continuous phase. All but one of the points are within a factor of 2 of the theoretical line. When this point is excluded, the average of the experimental values of $f_{La}/\sqrt{\tau}$ is 2.8 ± 0.7, compared with the theoretical value of 2.9 from Equation (19). The stagnant drop model appears to fit the data reasonably well. The turbulent drop model of Handlos and Baron predicts fractions extracted which vary from 0.45 at $\sqrt{\tau} = 2 \times 10^{-2}$ to 0.55 at $\sqrt{\tau} = 5 \times 10^{-2}$, which is not in accord either with the magnitude of the experimental results or the observed threefold variation in f_{La} over the experimental rang of τ. No information on the external coefficient can be obtained from the lanthanum data, since the extraction of this species is governed almost exclusively by transport within the drop. For the same reason, the additivity of

resistances assumption is valid for lanthanum extraction; there is practically no external resistance to be added in the sense of Equation (8).

The barium extraction data, on the other hand, should be representative of the external transfer process only, since the distribution coefficient of this species is smaller than that of lanthanum by a factor of nearly 50. Comparison of the barium data with Equation (16) shown in Figure 7 shows qualitative agreement between theory and experiment. The average of the experimental values of $f_{Ba}/(b_{Ba}\tau)$ [with Equation (9) used for the external resistance] is 2.3 ± 1.3. In accordance with Equation (16), this ratio should be 3. The barium fractions extracted are approximately an order of magnitude smaller than those for lanthanum which is in accord with the fiftyfold smaller distribution coefficient coupled with the factor of 5 difference between the internal and external coefficients. No information on the internal transfer process can be obtained from the barium data, since this process is completely masked by transfer in the continuous phase. The additivity assumption is also valid for barium extraction, since the $1/mk_e$ term in Equation (8) is much larger than the $1/k_i$ contribution.

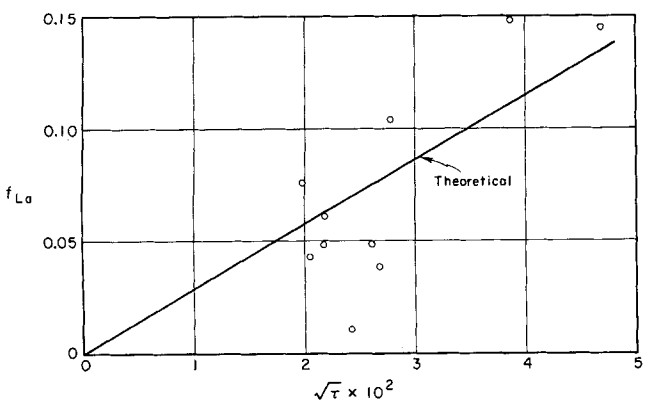

Fig. 7. Comparison of barium extraction results with molecular diffusion model with external resistance.

CONCLUSIONS

The proximity of the experimental internal coefficients to those predicted by molecular diffusion suggests that the drops were not oscillating or vibrating. However, some internal circulation must have existed in the falling drop. At Reynolds numbers much lower than those encountered here, the circulation pattern follows the Hadamard pattern which generates the mass transfer behavior demonstrated by Kronig and Brink (*11*). Johns and Beckmann (9) have investigated the transition from the stagnant diffusion limit to the Kronig and Brink limit as a function of the Peclet number, but for any Peclet number, the stagnant drop model is approached for sufficiently small contact times. The liquid metal system studied here was characterized by a combination of large Peclet number ($\sim 10^4$) and small τ ($10^{-4} - 10^{-3}$), and it is not possible to predict which limiting condition prevails, even if the circulation pattern were assumed to be that of Hadamard. However, the stagnant diffusion limit is probably approached for any internal circulation pattern as the contact time approaches zero. The penetration depth becomes so small that transport is no longer affected by the velocity gradients inside the drop. The contact times in the experiments reported here may have been sufficiently small to yield the rates characteristic of molecular diffusion, even though substantial circulation existed in the falling drop.

ACKNOWLEDGMENT

This work was supported by the Inorganic Materials Research Division of the Lawrence Radiation Laboratory under the auspices of the United States Atomic Energy Commission.

NOTATION

a = drop radius, cm.
a_{La} = activity (radioactive) of lanthanum-140 in the magnesium ingot
b = external resistance parameter, defined by Equation (12)
d = drop diameter, cm.
D = diffusion coefficient, sq. cm./sec.
f = fraction extracted
F = ratio of fraction of lanthanum to barium extracted
g = function defined by Equation (11)
k = individual mass transfer coefficient, cm./sec.
K = overall mass transfer coefficient defined by Equation (8), cm./sec.
m = concentration distribution coefficient
N = number of atoms
t = time, sec.
u = average fall velocity, cm./sec.
λ = decay constant, $sec.^{-1}$
τ = dimensionless time, Equation (13)

Subscripts and Superscript

e = external (continuous) phase
i = internal (drop) phase
La = lanthanum-140
Ba = barium-140
0 = immediately after extraction

LITERATURE CITED

1. Angelo, J. B., E. N. Lightfoot, and D. W. Howard, *AIChE J.*, **12**, 751 (1966).
2. Elzinga, R. B., Jr., and J. T. Banchero, *Chem. Eng. Progr. Symp. Ser. No. 29*, **55**, 199 (1959).
3. Garner, F. H., A. Foord, and M. Tayeban, *J. Appl. Chem.*, **9**, 315 (June, 1959).
4. Girifalco, L. A., and R. J. Good, *J. Phys. Chem.*, **61**, 094 (1957).
5. Griffith, R. M., *Chem. Eng. Sci.*, **12**, 198 (1960).
6. Handlos, A. E., and Thomas Baron, *AIChE J.*, **3**, 129 (1957).
7. Higbie, Ralph, *Trans. Am. Inst. Chem. Engrs.* **31**, 365 (1935).
8. Hu, Chengen, and R. C. Kintner, *AIChE J.*, **1**, 42 (1955).
9. Johns, L. E., Jr., and R. B. Beckmann, *ibid.*, **12**, 10 (1966).
10. Katz, H. M., F. B. Hill, and J. L. Speirs, *Trans. Am. Inst. Mining Engrs.*, **218**, 770 (1960).
11. Kronig, R., and J. C. Brink, *Appl. Sci. Res.*, **A2**, 142 (1950).
12. Ofte, Donald, unpublished manuscript.
13. Olander, D. R., *Nuc. Sci. Eng.*, **31**, 1 (1968).
14. ———, *AIChE J.*, **12**, 1018 (1966).
15. Newmen, A. B., *Trans. Am. Inst. Chem. Engrs.*, **27**, 203 (1931).
16. Pasternak, A. D., and D. R. Olander, *AIChE J.*, **13**, 1052 (1967).
17. Pasternak, A. D., *USAEC Rept. UCRL- 16108* (1966).
18. Patel, J. M., and R. M. Wellek, *AIChE J.*, **13**, 384 (1967).
19. Rose, D. M., and R. C. Kintner, *ibid.*, **12**, 530 (1966).
20. Wellek, R. M., A. K. Agrawal, and A. H. P. Skelland, *ibid.*, 854.

Manuscript received October 16, 1966; revision received June 12, 1967; paper accepted June 14, 1967.